HHS Public Access

Author manuscript

*Sci Signal*. Author manuscript; available in PMC 2019 March 18.

Published in final edited form as:

*Sci Signal*. ; 11(552): . doi:10.1126/scisignal.aat2214.

# Biased antagonism of CXCR4 avoids antagonist tolerance

**Ben Hitchinson**[1], **Jonathan M. Eby**[2], **Xianlong Gao**[2,3], **Francois Guite-Vinet**[4], **Joshua J. Ziarek**[5,6], **Hazem Abdelkarim**[1], **Youngshim Lee**[7], **Yukari Okamoto**[1], **Sojin Shikano**[1], **Matthias Majetschak**[2,3], **Nikolaus Heveker**[4], **Brian F. Volkman**[6], **Nadya I. Tarasova**[8], and **Vadim Gaponenko**[1,*]

[1]Department of Biochemistry and Molecular Genetics, University of Illinois at Chicago, Chicago, IL, USA.

[2]Department of Surgery, Burn and Shock Trauma Research Institute, Loyola University Chicago, Chicago, IL, USA.

[3]Department of Surgery, Morsani College of Medicine, University of South Florida, College of Medicine, Tampa, FL, USA.

[4]Department of Biochemistry, Research Centre, Sainte-Justine Hospital, Montréal, Quebec, Canada.

[5]Department of Molecular and Cellular Biochemistry, Indiana University, Bloomington, IN, USA.

[6]Department of Biochemistry, Medical College of Wisconsin, Milwaukee, WI, USA.

[7]Division of Bioscience and Biotechnology, Bio-molecular Informatics Center, Konkuk University, Seoul 05029, Republic of Korea.

[8]Cancer and Inflammation Program, National Cancer Institute, P.O. Box B, Frederick, MD, USA.

[*]Corresponding author. vadimg@uic.edu.

**Author contributions:** B.H. designed and performed chemotaxis, endocytosis, immunoprecipitation, Western blotting, cAMP ELISA, confocal microscopy, and NMR experiments. J.M.E. and X.G. performed the PRESTO-Tango assay. F.G.-V. performed the BRET assay. J.J.Z. performed the $Ca^{2+}$ flux experiments. H.A. helped with the identification of small molecule–biased antagonists. Y.L. performed the fluorescence spectroscopy. Y.O. and S.S. aided in the design of the endocytosis experiments. M.M. supervised the performance of the PRESTO-Tango assay and interpreted the results. N.H. designed and supervised the BRET experiments and helped with data interpretation. B.F.V. supervised the $Ca^{2+}$ flux studies and interpreted the results. N.I.T. discovered, developed, synthesized, and purified X4-2-6. V.G. conceived of the study. V.G. and B.H. interpreted the results. B.H., H.A., and V.G. wrote and edited the manuscript. All authors edited the final manuscript.

SUPPLEMENTARY MATERIALS

www.sciencesignaling.org/cgi/content/full/11/552/eaat2214/DC1

Fig. S1. AMD3100 increases CXCR4 abundance in Jurkat cells.
Fig. S2. Neither AMD3100 nor X4-2-6 causes CXCR4 internalization.
Fig. S3. AMD3100 but not X4-2-6 inhibits CXCL12-stimulated CXCR4 endocytosis.
Fig. S4. BA2 recruitment downstream of CXCR4 is not substantially affected by X4-2-6.
Fig. S5. X4-2-6 does not inhibit BA2 recruitment to CXCR4.
Fig. S6. BA1/2 regulates ERK phosphorylation downstream of CXCR4.
Fig. S7. CXCR4 and CCR2 share 63% amino acid sequence similarity in the region of the receptor corresponding to X4-2-6.
Fig. S8. X4-2-6 inhibits the CXCL12-mediated chemotaxis of THP-1 cells.
Fig. S9. X4-2-6 binds directly to CXCL12.
Fig. S10. AMD3100 displaces the N terminus of CXCL12 from the binding site of CXCR4.
Fig. S11. The small molecule SEN071 is a biased antagonist of CXCR4 that avoids antagonist tolerance.

**Competing interests:** N.I.T. is a co-inventor on a patent application filed by the NIH/NCI for the X4-2-6 peptide. B.F.V. has an ownership interest in Protein Foundry LLC. The other authors declare that they have no competing interests.

**Data and materials availability:** All data needed to evaluate the conclusions in the paper are present in the paper or the Supplementary Materials.

## Abstract

Repeated dosing of drugs targeting G protein–coupled receptors can stimulate antagonist tolerance, which reduces their efficacy; thus, strategies to avoid tolerance are needed. The efficacy of AMD3100, a competitive antagonist of the chemokine receptor CXCR4 that mobilizes leukemic blasts from the bone marrow into the blood to sensitize them to chemotherapy, is reduced after prolonged treatment. Tolerance to AMD3100 increases the abundance of CXCR4 on the surface of leukemic blasts, which promotes their rehoming to the bone marrow. AMD3100 inhibits both G protein signaling by CXCR4 and β-arrestin1/2–dependent receptor endocytosis. We demonstrated that biased antagonists of G protein–dependent chemotaxis but not β-arrestin1/2 recruitment and subsequent receptor endocytosis avoided tolerance. The peptide antagonist X4-2-6, which is derived from transmembrane helix 2 and extracellular loop 1 of CXCR4, limited chemotaxis and signaling but did not promote CXCR4 accumulation on the cell surface or cause tolerance. The activity of X4-2-6 was due to its distinct mechanism of inhibition of CXCR4. The peptide formed a ternary complex with the receptor and its ligand, the chemokine CXCL12. Within this complex, X4-2-6 released the portion of CXCL12 critical for receptor-mediated activation of G proteins but enabled the rest of the chemokine to recruit β-arrestins to the receptor. In contrast, AMD3100 displaced all components of the chemokine responsible for CXCR4 activation. We further identified a small molecule with similar biased antagonist properties to those of X4-2-6, which may provide a viable alternative to patients when antagonist tolerance prevents drugs from reaching efficacy.

## INTRODUCTION

G protein–coupled receptors (GPCRs) belong to the largest family of membrane proteins in the human body and direct most physiological processes in health and disease (1–3). Hence, GPCRs are targeted by almost 35% of all current therapeutics (4). Unfortunately, cells often become tolerant to the effects of these drugs. Tolerance is associated with the reduced efficacy of a compound after its repeated administration. Examples of this phenomenon include tolerance to opioid receptor agonists that activate receptors for pain relief and tolerance to dopamine D2 receptor antagonists that inhibit the receptor in the treatment of schizophrenia (5–9). The exact mechanisms that cause tolerance are unclear. Many studies have highlighted altered receptor abundance at the cell surface as a possible mechanism for the reduced efficacy of GPCR-targeting drugs (5, 6, 10, 11). Currently, no studies provide a strategy to avoid the development of antagonist tolerance.

Tolerance to the U.S. Food and Drug Administration–approved CXCR4 receptor antagonist AMD3100 can occur (11). This tolerance is associated with increased receptor expression on the cell surface. CXCR4 is a chemokine receptor that functions in a large number of processes, including embryonic development (12), the homing and maintenance of hematopoietic stem cells (13–16), and immune cell chemotaxis toward its cognate ligand CXCL12 (17, 18). CXCR4 overexpression is observed in 23 different cancer types, where it is associated with a highly metastatic phenotype (19). Despite its potentially broad application to many disease conditions, AMD3100 is only used to mobilize stem cells from the bone marrow for transplantation (20). On the basis of this function, AMD3100 may be expected to mobilize leukemic blasts, which are progenitor cells responsible for leukemia

relapse, from the bone marrow into the peripheral blood of patients with leukemia to make the cells more easily eliminated by chemotherapy. However, after prolonged treatment with this compound, leukemic blasts can become tolerant to the drug and rehome to the bone marrow where they are protected from cytotoxic drug exposure (11, 21). This suggests that, for applications requiring prolonged dosing, tolerance to receptor antagonists can substantially limit their therapeutic potential. AMD3100 is an unbiased antagonist that inhibits G protein signaling and the β-arrestin1/2 (BA1/2)–dependent endocytosis of CXCR4 with equal potency (22). β-arrestin1 (BA1) and β-arrestin2 (BA2), also known as arrestins 2 and 3, interact with the phosphorylated intracellular sites on active CXCR4 and engage clathrin to promote receptor endocytosis (23). Prolonged exposure to AMD3100 promotes the accumulation of CXCR4 on the surface of leukemia cells, as is observed in other models of antagonist tolerance (5–9), enabling the chemo-taxis of cells to CXCL12 even in the presence of the drug (11).

Here, we hypothesized that antagonists that inhibited G protein signaling but not receptor endocytosis might avoid the development of tolerance. Few compounds of this type, called biased antagonists, have been discovered (24–27). We found that a peptide derived from transmembrane helix 2 (TM2) and extracellular loop 1 (ECL1) of CXCR4, named X4-2-6, acted as a biased antagonist of the receptor that inhibited G protein signaling but not the recruitment of BA1/2 to the receptor. Whereas AMD3100 was a competitive orthosteric antagonist of CXCR4, X4-2-6 acted through a different mechanism. X4-2-6 formed a ternary complex with CXCR4 and CXCL12 that disrupted the interaction of the receptor with the extreme N terminus of the chemokine, which is crucial for G protein activation by the receptor (28–32). At the same time, the portion of CXCL12 that is important for BA1/2 recruitment and function was free to bind to CXCR4. These differences in the mechanisms of inhibition between AMD3100 and X4-2-6 resulted in the receptor not accumulating on the cell surface in the presence of the peptide and prevented the subsequent development of tolerance. In addition, we showed that the avoidance of tolerance was not limited to peptide-biased antagonists but could also be achieved with a small molecule–biased antagonist called SEN071 (24). We propose that biased antagonists of GPCRs may provide advantages to patients who develop tolerance to unbiased antagonist drugs.

## RESULTS

### Inhibition of CXCR4 endocytosis results in the development of antagonist tolerance

Although both AMD3100 and X4-2-6 abate metastasis and reduce tumor burden, X4-2-6 prolongs patient survival (33), whereas AMD3100 does not (34). Although the potency of AMD3100 may have decreased over time (11), it remained possible that X4-2-6 maintained its inhibitory activity by acting through a distinct mechanism. When we tested this hypothesis by comparing the potency of AMD3100 and X4-2-6 aGαinst CXCR4-mediated chemotaxis of Jurkat T lymphocytic leukemia cells without pretreatment, we found that without preexposure, AMD3100 inhibited chemotaxis with a median inhibitory concentration ($IC_{50}$) of 0.7 ± 0.2 μM. However, 72 hours of preexposure can promote the tolerance of several leukemia cell lines to AMD3100, which paradoxically increases chemotaxis to CXCL12 in the presence of the antagonist (11). Consistent with this, we

found that cells preexposed to AMD3100 for 72 hours became tolerant to this antagonist, which was reflected by a nearly fourfold increase in the $IC_{50}$ value for the inhibition of CXCL12-mediated chemotaxis (Fig. 1A). More severe tolerance developed after preexposure to a greater concentration of AMD3100, which further increased the $IC_{50}$ value. However, X4-2-6 preexposure did not promote antagonist tolerance, resulting in similar $IC_{50}$ values before or after preexposure for 72 hours, respectively (Fig. 1A). Thus, prolonged exposure of cells to AMD3100 decreased the potency of the drug, consistent with antagonist tolerance, whereas no tolerance was observed with X4-2-6 (Fig. 1A).

Antagonist tolerance is correlated with the increased cell surface expression of the target receptor (11, 35). We treated cells with AMD3100 or X4-2-6 for up to 72 hours and compared the abundance of cell surface CXCR4 to cells treated only with vehicle. Consistent with our earlier observations (Fig. 1A), treatment with AMD3100 for 72 hours increased cell surface CXCR4 expression when compared to that of vehicle-treated cells (Fig. 1B) and increased the total CXCR4 protein amount (fig. S1). Conversely, treatment of Jurkat cells with X4-2-6 for 72 hours had no effect on CXCR4 cell surface expression (Fig. 1B). This may be because AMD3100 inhibited CXCL12-mediated receptor internalization, whereas X4-2-6 neither efficiently inhibited nor promoted this process (Fig. 1C and figs. S2 and S3). This is consistent with the reported inhibition of endocytosis by AMD3100 (22) and with the internalization of X4-2-6 with the receptor after CXCL12 stimulation (33).

Our findings suggest that inhibition of endocytosis may increase CXCR4 cell surface expression and lead to the development of tolerance. We tested this hypothesis by treating cells with the dynamin inhibitor dynasore, which blocks clathrin-mediated receptor endocytosis, a principal mechanism of CXCR4 internalization (23). Treatment with dynasore for 1 hour increased CXCR4 cell surface expression (Fig. 1D). The increased amount of CXCR4 on the cell surface correlated with the reduced potency of AMD3100 to inhibit chemotaxis to CXCL12 (Fig. 1D). This observation correlated the inhibition of endocytosis by either AMD3100 or dynasore with receptor accumulation on the cell surface and the subsequent development of antagonist tolerance. If receptor endocytosis was not inhibited, then antagonist tolerance did not develop, and antagonists maintained their efficacy.

### X4-2-6 does not inhibit BA1/2 downstream of CXCR4

CXCR4 endocytosis is largely regulated by BA1/2, scaffolding proteins recruited to the receptor upon stimulation by CXCL12 (36). In Jurkat cells at rest, confocal microscopy showed that CXCR4 populated both the cell membrane and internal compartments, whereas BA2 was abundant in the cytoplasm (Fig. 2A and fig. S4). Colocalization of CXCR4 and BA2 in intracellular punctate structures was observed in CXCL12-stimulated cells (Fig. 2A and fig. S4). X4-2-6 did not alter the CXCL12-mediated colocalization of CXCR4 with BA2 or receptor internalization (Fig. 2A and fig. S4). However, AMD3100 inhibited both CXCR4 endocytosis and its colocalization with BA2 (Fig. 2A and fig. S4). The effects of antagonists on the recruitment of BA2 to CXCR4 were also monitored using a PRESTO-Tango (parallel receptorome expression and screening by transcriptional output, with transcriptional activation following arrestin translocation) assay in which GAL4-VP16 attached to the

receptor was released byrecruitment of the BA2–tobacco etch virus pro-tease fusion, which activated the transcription of a b-lactamase reporter gene (37). CXCL12-dependent BA2 recruitment was unaffected by X4-2-6, whereas AMD3100 increased the $EC_{50}$ (median effective concentration) value more than 3500-fold (Fig. 2B). Bioluminescence resonance energy transfer (BRET) between CXCR4 and BA2 further supported the finding that X4-2-6 did not inhibit BA2 recruitment (fig. S5).

To enhance BA1/2 recruitment and receptor endocytosis, serine residues in the CXCR4 C terminus are phosphorylated by several kinases, such as GPCR kinases (GRKs), protein kinase C (PKC), and proviral integration site Moloney murine leukemia virus-1 kinase (PIM1) (23, 38). When we used Western blotting to detect the phosphorylation of $Ser^{324/325}$ or $Ser^{339}$ in the C terminus of CXCR4, we found that AMD3100 inhibited this posttranslational modification, but X4-2-6 had had no effect (Fig. 2C). Together, these data suggest that X4-2-6 was distinct from AMD3100 in its inability to affect receptor phosphorylation, BA2 recruitment, endocytosis of CXCR4, and CXCR4 abundance on the plasma membrane, which correlated with the avoidance of antagonist tolerance.

Inefficient inhibition of BA1/2 signaling may also suggest the poor activity of X4-2-6 aGαinst CXCR4, although this antagonist binds to and inhibits this receptor (33, 39, 40). We therefore investigated the effects of X4-2-6 on the generation of phosphorylated extracellular signal–regulated kinase 1/2 (pERK1/2) at $Thr^{202}$ and $Tyr^{204}$, a process that involves both G protein signaling and BA1/2 regulation (41–43). As expected (44), pERK1/2 abundance was maximal after 5 min of treatment with CXCL12 and was maintained for up to 30 min after treatment with the chemokine (Fig. 2, D and E). Knockdown of BA1/2 in Jurkat cells increased both the early and late peaks in pERK1/2 abundance compared to Jurkat cells electroporated with scrambled small interfering RNA (siRNA) controls (fig. S6, A and B). Treatment with barbadin, an inhibitor of BA1/2 binding to the β-adaptin subunit of adaptor protein 2 (AP2) (45), also increased the early and late peaks in pERK1/2 abundance compared to vehicle-treated cells (fig. S6C). A similar result was observed in mouse embryonic fibroblasts (MEFs) lacking BA1/2 expression (46) but not in wild-type (WT) MEFs (fig. S6, D and E). These data suggest that the phosphorylation of ERK1/2 downstream of CXCR4 stimulation was due to G protein signaling, whereas BA1/2 played a role in desensitization and inhibition of late G protein–mediated signaling, as was previously observed (44). Whereas X4-2-6 reduced the early phase of ERK1/2 phosphorylation, ERK1/2 activation was sustained similar to that in vehicle-treated cells (Fig. 2, D and E). In contrast, AMD3100 inhibited both early and late peaks in pERK1/2 generation in Jurkat cells stimulated with CXCL12 (Fig. 2, D and E). Thus, X4-2-6 inhibited the G protein-mediated activation of ERK1/2.

## X4-2-6 is a biased antagonist that specifically inhibits G protein activation downstream of CXCR4

Because X4-2-6 inhibited chemotaxis, a process associated with G protein signaling, but did not affect BA1/2 recruitment, we reasoned that X4-2-6 might act as a biased antagonist of CXCR4. Amplification of signaling leading to pERK1/2 generation can potentially obscure the analysis of bias in X4-2-6. To study the direct effect of the antagonist on G proteins, we

Immunoprecipitated guanosine triphosphate–bound Gαi (Gαi-GTP) and analyzed by Western blotting in lysates of Jurkat cells treated with CXCL12 in the presence of vehicle, AMD3100, or X4-2-6. CXCL12 increased the abundance of Gαi-GTP compared to that in unstimulated control cells (Fig. 3, A and B). Either AMD3100 or X4-2-6 reduced the amount of Gαi-GTP in CXCL12-treated cells (Fig. 3, A and B). To assess the effect of the antagonists on the function of Gαi-GTP, we measured the abundance of the second messenger cAMP (cyclic adenosine monophosphate) in CXCL12-stimulated Jurkat cells in the presence or absence of either AMD3100 or X4-2-6. Treatment with forskolin, which stimulates adenylate cyclase to generate cAMP (47), increased intracellular cAMP amounts when compared to those of vehicle-treated cells, which were reduced by CXCL12 through the inhibitory action of Gαi on adenylate cyclase (Fig. 3C). Both AMD3100 and X4-2-6 returned cAMP amounts to those observed in cells treated with forskolin alone (Fig. 3C). In addition, X4-2-6 inhibited CXCL12-mediated chemotaxis in a dose-dependent manner (Fig. 3D). Thus, similar to AMD3100, X4-2-6 inhibited the activation and function of Gαi downstream of CXCR4. These data suggest that, whereas AMD3100 acts as an unbiased antagonist of CXCR4, X4-2-6 is a biased antagonist, which inhibits G protein signaling but not BA1/2 recruitment.

To confirm that this biased antagonism was due to the specific activity of X4-2-6, we compared the effects of the peptide on CXCR4- and CCR2-mediated $Ca^{2+}$ flux, which is initiated by G proteins through their activation of phospholipase C (48). The receptors CXCR4 and CCR2 share 63% sequence identity in the region corresponding to X4-2-6 (fig. S7). We found that X4-2-6 inhibited $Ca^{2+}$ flux stimulated by CXCL12 (Fig. 3E) but not by the CCR2 ligand CCL2 (Fig. 3F) in Tohoku Hospital Pediatrics-1 (THP-1) human monocytic leukemia cells, which express both receptors. These data demonstrated the specificity of the peptide for CXCR4. X4-2-6 also inhibited the CXCL12-dependent chemotaxis of the same cells (fig. S8).

## X4-2-6 simultaneously binds to CXCL12 and CXCR4to function as a biased antagonist

The peptide sequence of X4-2-6 is derived from CXCR4 (39). Thus, its biased antagonism might arise from a direct interaction with CXCL12. The tertiary structure of CXCL12 is similar to that of other chemokines with a flexible N terminus and an extended N-loop (49), which is connected through a $3_{10}$ helix to the “globular portion” of the chemokine that consists of a three-stranded α sheet. The CXCL12 N terminus is crucial for binding to and activating CXCR4 (28–32, 50), whereas the globular portion of the chemokine interacts with the receptor N terminus (17, 51). We observed statistically significant signal attenuation in the heteronuclear single-quantum coherence nuclear magnetic resonance (HSQC NMR) spectra of $^{15}$N-labeled CXCL12 in the presence of X4-2-6 for the residues $Phe^{14}$, $Ser^{16}$, and $His^{17}$ in the N-loop of the chemokine. This indicates the binding of X4-2-6 to the N-loop of the chemokine (Fig. 4, A to C). The interaction was further corroborated by tryptophan fluorescence experiments, which showed a statistically significant change in maximal tryptophan fluorescence and intensity upon X4-2-6 binding to CXCL12 (fig. S9). Because the CXCL12 N terminus is crucial for binding to and activating CXCR4 (28–32, 50), NMR signals corresponding to the N-terminal residues of $^{15}$N-labeled CXCL12 (for example, $Ser^{4}$ and $Leu^{5}$) were reduced after the addition of CXCR4-expressing cell membranes (Fig. 4, D

to F). Residues in the globular domain of the chemokine (Ala[35], Asn[46], and Lys[54]) were also affected, suggesting a larger interaction interface between the chemokine and the receptor compared to CXCL12 and X4-2-6. CXCR4-containing membranes, together with X4-2-6, substantially reduced the NMR signals from residues within the β1 and β2 strands of CXCL12 (Fig. 4, G to I). The addition of CXCR4-expressing membranes together with X4-2-6 did not recapitulate the chemokine spectra with CXCR4 or peptide alone, which may suggest that both the receptor and the peptide bind to the chemokine simultaneously. Although Leu[5] of CXCL12 was undetectable by NMR analysis of CXCR4 alone, a weak signal was observed with the combination of the membrane and peptide. This suggests that, by forming a ternary complex with the chemokine and receptor, X4-2-6 partially liberated the extreme N-terminal portion of CXCL12. In contrast, AMD3100 decreased the affinity of the entire N terminus of CXCL12 for CXCR4, as evidenced by fast solvent exchange between the free and bound species for the N-terminal residues Ser[4], Ser[6]-Arg[8], Arg[12], Ser[16], and His[17], as well as Lys[27], Val[39], Lys[56], and Leu[66], in the globular portion of the chemokine (fig. S10), as was expected (29). Our results are consistent with the notion that the extreme N-terminal region of the chemokine is more critical for chemotaxis than for receptor endocytosis (52) and suggest a previously unknown mechanism of biased antagonism. Moreover, our findings may explain how the specificity of peptides derived from the transmembrane domains of their targets might be enhanced by additional interactions with the receptor.

### A small molecule–biased antagonist of CXCR4 also avoids the development of tolerance

We investigated whether the avoidance of antagonist tolerance was a unique property of X4-2-6 or whether tolerance could be generally evaded by biased antagonists. A small molecule–biased antagonist of CXCR4, SEN071, which is unrelated to X4-2-6, was previously described (24). We found that concentrations of SEN071 that inhibited the chemotaxis of Jurkat cells to CXCL12 did not prevent CXCR4 endocytosis (fig. S11A). Similar to X4-2-6, SEN071 exhibited similar $IC_{50}$ values for CXCL12-induced chemotaxis with and without pre-exposure to the compound (fig. S11B) and did not increase the abundance of CXCR4 on the cell surface (fig. S11A). Thus, both peptide- and small molecule–biased antagonists that avoid accumulation of the receptor on the cell surface did not promote antagonist tolerance after prolonged exposure times.

## DISCUSSION

Antagonist tolerance correlates in part with accumulation of the target receptor on the cell surface (5–7, 9, 11). Some examples include overexpression of β-adrenergic receptors in response to prolonged treatment with their antagonists propranolol and nadolol (10, 53), the increased abundance of α1A and α1D adrenergic receptors after prolonged exposure to their inhibitors prazosin and terazosin (8, 9), and the increased expression of the dopamine D2 receptor after chronic treatment with the antipsychotic antagonists haloperidol and perphenazine (7). Accelerated trafficking to the plasma membrane and increased expression of the receptor have been suggested as potential mechanisms for its accumulation after repeated dosing with antagonists (10). Our results showed that prolonged exposure of cells to AMD3100 led to the increased cell surface expression of its primary target and

development of antagonist tolerance consistent with previous observations of CXCR4 (11, 21) and other GPCRs (8, 35, 53).

CXCR4 in T lymphocytes undergoes slow constitutive internalization at a rate of about 1% of cell surface receptor per minute (54). AMD3100 inhibits this process and leads to accumulation of the receptor on the cell surface (22). Our experiments with the inhibitor of endocytosis dynasore suggest that blocking receptor endocytosis was sufficient to induce tolerance to the drug (Fig. 1D). Expedited trafficking of CXCR4 to the plasma membrane, its accelerated expression, or reduced degradation in response to AMD3100 might contribute to the increased abundance of the receptor on the plasma membrane and antagonist tolerance. Our data suggest that biased antagonists that inhibit G protein signaling but not receptor endocytosis might be used to avoid antagonist tolerance.

Our investigation revealed that X4-2-6, a peptide analog of the TM2 and ECL1 of CXCR4 (33), is a biased antagonist. Unlike AMD3100, the peptide at its $IC_{50}$ did not prevent the C-terminal phosphorylation of CXCR4 (Fig. 2C), subsequent recruitment of BA1/2 (Fig. 2B), and receptor endocytosis (figs. S2 and S3) in response to stimulation with CXCL12. Similar to AMD3100, X4-2-6 blocked the GTP loading of Gαi (Fig. 3A), inhibited the CXCL12-dependent modulation of cAMP production (Fig. 3C), reduced the early phase of pERK1/2 generation (Fig. 2D), curtailed $Ca^{2+}$ flux (Fig. 3E), and prevented chemotaxis toward CXCL12 (Fig. 3D). Inhibition of $Ca^{2+}$ flux by X4-2-6 is expected to reduce the activity of PKC, a kinase that phosphorylates $Ser^{324/325}$ in CXCR4 (55). However, these residues can also be phosphorylated in Jurkat cells by PIM1 (56). Alternatively, GRK2 and GRK6 phosphorylate $Ser^{324/325}$ in CXCR4 in human embryonic kidney (HEK) 293 cells (23, 55). In Jurkat cells, which also express GRK6, 50% of GRK2 is degraded 1 hour after stimulation with CXCL12 (57, 58). Thus, whereas X4-2-6 might prevent PKC from phosphorylating CXCR4, other kinases may potentially act as substitutes.

CXCL12 activates G proteins downstream of CXCR4 to phosphorylate ERK1/2 (59). Sustained ERK1/2 activation after more than 30 min of stimulation with the chemokine may be due to G protein–mediated activation of the Ras-Raf pathway or the scaffolding function of BA1/2 (42, 59, 60). The relative contributions of G proteins and BA1/2 to the late phase of pERK1/2 generation vary in different GPCRs (61). For example, in the context of the angiotensin AT1a receptor, BA1/2 promotes ERK1/2 phosphorylation (62), whereas G protein signaling is responsible for the activation of ERK1/2 downstream of the M3 muscarinic receptor (63) and BA1/2 plays a regulatory role (64). Our experiments in BA1/2-deficient MEFs suggest that the primary function of BA1/2 is to promote receptor desensitization and to prevent excessive phosphorylation of ERK1/2 in response to CXCR4 stimulation (fig. S6). The fact that treatment with barbadin, which inhibits the association of arrestin with the β-adaptin subunit of AP2, also increased the abundance of pERK1/2 in CXCL12-stimulated cells suggests that these kinases are regulated by receptor internalization rather than by recruitment of BA1/2. Our results are consistent with studies showing that BA1/2 knockdown in HeLa cells and MEFs increases pERK1/2 abundance in response to CXCL12 (44) and interleukin-8 (65). Moreover, our findings are consistent with those of a study that used CRISPR-Cas9–mediated deletion of multiple Ga proteins and BA1/2 to demonstrate that a broad set of GPCRs engage G proteins but not arrestins to

initiate ERK signaling (66). However, BA1/2 are required for CXCR4-dependent pERK1/2 generation in HEK 293 cells (42, 67), which suggests that BA1/2 might have a complex and cell type–specific role in CXCR4 signaling.

The differences in the mechanisms of inhibition between AMD3100 and X4-2-6 may be due to the distinct interactions of the antagonists with the receptor and the chemokine (Fig. 5, A to C). The peptide agonist X4-2-6 interacts with both CXCL12 and CXCR4 simultaneously to form a ternary complex. We found that within the ternary complex, the interaction between the receptor and the peptide caused the extreme N terminus of the chemokine to become detached from CXCR4 (Fig. 5B). This portion of CXCL12 is implicated in inducing the conformation of the receptor that promotes the GTP loading of Gαi (52). Thus, the interaction with X4-2-6 may prevent conformational transitions in CXCR4 that lead to the activation of G proteins but enable phosphorylation of the receptor C terminus and the recruitment of BA1/2. We found that X4-2-6 decreased the early peak in pERK1/2 abundance in Jurkat cells by inhibiting G protein activation but enabled BA1/2 recruitment to the receptor and subsequent regulation of the phosphorylation of both isoforms of this kinase. This contrasts with AMD3100, which interacts with the receptor and reduces CXCL12 binding by displacing its entire N terminus from CXCR4. In our studies, AMD3100 treatment potently suppressed early and late pERK1/2 generation. The residual weak binding of CXCL12 to the receptor-AMD3100 complex could be mediated by the globular domain of the chemokine, which is less affected by the drug (29). Although at high concentrations AMD3100 can become a partial agonist of CXCR4 (68), X4-2-6 does not exhibit a similar activity (Figs. 1C and 3D). Because ERK1/2 signaling in T lymphocytes is important for survival, the different modes of receptor binding exhibited by X4-2-6 and AMD3100 might also differentially affect cell viability (69).

The binding of X4-2-6 to CXCL12 involves the N-loop of the chemokine. This binding site cannot be predicted on the basis of the amino acid sequence of the peptide corresponding to TM2 and ECL1 of CXCR4. The current model for the interaction of CXCL12 with CXCR4 suggests that $Lys^{25}$ in the N terminus of the receptor binds to the N-loop region of the chemokine (30). The amino acid sequence of X4-2-6 does not have lysine residues (33). However, X4-2-6 contains two (non-native to CXCR4) C-terminal aspartates and amidated polyethylene glycol that can generate or modify a binding site for the chemokine within the peptide. In addition, the tertiary structure of X4-2-6 is different from the structure of the corresponding region in CXCR4, and this might expose a novel site for interaction with CXCL12 (33).

Our proposed mechanism for the biased antagonism of CXCR4 differs from the model for the cholecystokinin receptor (26), which suggests the existence of different conformational states of receptors. This previous model predicts that antagonists selectively interact with G protein–activating conformers but not BA1/2-activating conformers of the receptor (26). However, in our studies, X4-2-6 interacted with receptors on the cell surface and with those that were endocytosed, regardless of receptor conformation (33). Thus, multiple mechanisms of biased antagonism are possible.

Future pharmaceutical development will likely benefit from understanding how new treatments can avoid the development of tolerance. We found that a small molecule–biased antagonist acted similarly to a peptide-biased antagonist to avoid tolerance, which suggests that flexibility in the design of such agents is possible. Currently, very few biased antagonists have been characterized, and the advantages of biased antagonists in general remain an unexplored avenue for drug discovery (24–27). Our study suggests that biased antagonists can potentially provide therapeutic options to patients who develop tolerance to unbiased antagonists.

## MATERIALS AND METHODS

### Antibodies

Western blotting was performed with antibodies from the following sources: BA1/2 (clone D24H9, #4674; Cell Signaling), CXCR4 (clone UMB2, AB124824; Abcam), CXCR4 (SAB3500383; Sigma-Aldrich), CXCR4 pSer$^{324/325}$ (CP4251, ECM Biosciences), CXCR4 pSer$^{339}$ (SAB4504153; Sigma-Aldrich), ERK1/2 (9102; Cell Signaling), pERK1/2 (9101; Cell Signaling), total Gαi (AB102014; Abcam), GAPDH (60004–1-Ig; Proteintech), rabbit anti-mouse (7076; Cell Signaling), and mouse anti-rabbit (7074; Cell Signaling). Confocal microscopy was performed using antibodies from the following sources: BA2 (clone C16D9, #3857; Cell Signaling), CXCR4 (clone UMB2, AB124824; Abcam), Alexa Fluor 488 goat anti-rabbit (R37116; Thermo Fisher Scientific), Alexa Fluor 555 goat anti-mouse (A21422; Thermo Fisher Scientific). For flow cytometry, staining was performed using antibodies from the following sources: PE-tagged CXCR4 4G10 monoclonal antibody (clone 4G10, sc-53534PE; Santa Cruz Biotechnology), PE-tagged CXCR4 12G5 monoclonal antibody (clone 12G5, 306506; BioLegend), PE- Mouse IgG2b, κ Isotype control antibody (402204; BioLegend), and PE-Mouse IgG2a, κ Isotype control antibody (400212; BioLegend). For immunoprecipitation, 1 μl of anti-active Gαi (26901;New East Biosciences)was used per 500 μl of sample.

### BRET assays

BA2 recruitment to CXCR4 was measured by BRET. Briefly, the BRET signal was measured in cells cotransfected with 1.0 μg of BA2-GFP10 and 0.05 mg of CXCR4-Rluc or 0.05 mg of CXCR4-Rluc, normalized to 2 μg per well with empty vector. BA2 recruitment was assessed by adding the ligands 10 min after the addition of coelenterazine 400A.

### Analysis of cAMP concentration by ELISA

Jurkat cells ($5 \times 10^6$) were serum-starved for 6 hours in RPMI 1640, 1% penicillin-streptomycin, and 2 μM L-glutamine and then stimulated with 100 μM forskolin or vehicle for 30 min. Each sample was then treated with vehicle or CXCR4 antagonists, where indicated, for 30 min. Cells were exposed to 30 nM CXCL12 for a further period of 30 min. A direct cAMP ELISA kit (Enzo Life Sciences) was used to measure cAMP concentrations in cell lysates. The relative change in cAMP concentration was calculated using Assay Blaster! Software (ADI-28–0002), and the results were plotted with GraphPad Prism 7.00 (GraphPad Software) to determine the effects of CXCR4 inhibitors on cAMP production in response to CXCL12.

### Measurement of $Ca^{2+}$ flux

THP-1 cells ($2 \times 10^5$) were incubated for 1 hour with the indicated concentration of X4-2-6. Each sample contained Hanks' balanced salt solution (HBSS), 20 μM Hepes (pH 7.4), 0.1% bovine serum albumin (BSA), 5% (v/v) phosphate-buffered saline (PBS), 0.125% (v/v) dimethyl sulfoxide (DMSO), and Calcium4 $Ca^{2+}$-sensitive fluorophore (Molecular Devices). Baseline fluorescence was measured for 20 s before the cells were exposed to 10 nM CXCL12, and the response was measured for an additional 60 s. The percentage baseline $Ca^{2+}$ response was calculated by subtracting the baseline fluorescence from the peak fluorescence.

### Cell culture

Jurkat, THP-1, and Chinese hamster ovary K1 (CHO-K1) cells were obtained from the American Type Culture Collection. MEFs were a gift from the Lefkowitz Lab. Jurkat cells were cultured in suspension, in culture medium consisting of RPMI 1640 (Sigma-Aldrich) supplemented with 10% heat-inactivated fetal bovine serum (FBS; Sigma-Aldrich), 1% penicillin-streptomycin (Thermo Fisher Scientific) solution, and a final concentration of 2 μM L-glutamine (Thermo Fisher Scientific). For serum starvation, Jurkat cells were cultured in medium consisting of RPMI 1640 supplemented with 1% penicillin-streptomycin and a final concentration of 2 μM L-glutamine. THP-1 cells were cultured in RPMI 1640 containing 10% FBS (Sigma-Aldrich), 1% penicillin-streptomycin, and 0.05 μM 2-mercaptoethanol (Thermo Fisher Scientific). CHO-K1 cells cultured in F-12K medium (Gibco) containing 10% FBS and 1% penicillin-streptomycin. MEFs were cultured in medium consisting of Dulbecco's modified Eagle's medium (DMEM; Gibco) supplemented with 10% FBS (Sigma-Aldrich), 1% penicillin-streptomycin (Thermo Fisher Scientific), and a final concentration of 2 μM L-glutamine (Thermo Fisher Scientific). For serum starvation of MEFs, cells were cultured in medium consisting of DMEM supplemented with 1% penicillin-streptomycin and a final concentration of 2 μM L-glutamine. All cells were maintained in a humidified environment containing 5% $CO_2$ at 37°C.

### Chemotaxis assay

Jurkat cells were maintained in migration medium consisting of RPMI 1640, 2 μM L-glutamine, 20 μM Hepes (pH 7.4) (Thermo Fisher Scientific) and 0.1% fraction V BSA (Thermo Fisher Scientific) for 6 hours before the start of the assay. Cells were preincubated with vehicle or CXCR4 antagonists for 30 min before $1 \times 10^5$ cells were seeded into the upper chamber of a 5-μm-pore Transwell plate (Corning). Cells were stimulated to migrate toward the lower chamber by migration medium containing 30 nM CXCL12. After 2.5 hours, cells in the lower chamber were counted using a Beckman Coulter flow cytometer, and data were plotted using GraphPad Prism 7.00 (GraphPad Software).

### Confocal microscopy

Jurkat cells ($1 \times 10^5$) were serum-starved for 6 hours and then treated with CXCR4 inhibitors for 30 min before stimulation with 30 nM CXCL12 for 60 min. Cells were then pelleted by centrifugation and fixed in 4% formaldehyde. Cells were pelleted, washed, and resuspended in PBS. Onto a poly-lysine–coated coverslip, 5 μl of cell suspension was

smeared using a pipette tip. The sample was then blocked in PBS containing 5% BSA and 0.3% Triton X-100 for 1 hour at room temperature, before incubation overnight with a mouse monoclonal anti-CXCR4 and rabbit monoclonal anti–BA2 antibody at 4°C in the same buffer. Coverslips were washed with ice-cold PBS and then stained with anti-rabbit Alexa Fluor 488 and anti-mouse Alexa Fluor 555 secondary antibodies for 1 hour at room temperature. Last, coverslips were incubated with DAPI (0.5 μg/ml; D1306; Thermo Fisher Scientific) for 10 min before being washed three times in PBS. Coverslips were mounted onto slides with ProLong Gold Antifade Reagent (Thermo Fisher Scientific) and analyzed on a Zeiss laser scanning 710 microscope.

### CXCR4 ligand and antagonist preparation

CXCL12 (Protein Foundry) was prepared in PBS. To prepare stock concentrations of peptides, 2 mg of lyophilized X4-2-6 was incubated in a volume of DMSO that would represent 5% of the final volume of solution at 37°C for 30 min. The peptide was diluted to the final stock concentration using PBS before being applied to cells. AMD3100 octahydrochloride hydrate (Sigma-Aldrich) was prepared in PBS and SEN071 (MolPort) in DMSO.

### CXCR4 phosphorylation assay

Jurkat cells ($1 \times 10^6$) were serum-starved for 6 hours before treatment with vehicle, 1 μM AMD3100, or 10 μM X4-2-6 for 30 min. Cells were then stimulated with 30 nM CXCL12 for 30 min before harvesting and lysis in ice-cold radioimmunoprecipitation assay (RIPA) buffer. CXCR4 phosphorylation was analyzed after SDS–polyacrylamide gel electrophoresis (SDS-PAGE) and Western blotting.

### Dynasore treatment

Jurkat cells were serum-starved for 6 hours before treatment for 1 hour with 80 μM dynasore (Sigma-Aldrich) and then were washed three times with PBS. Cells were then prepared for the appropriate assays. Cell surface expression of CXCR4 was measured using anti-CXCR4-PE antibody clone 4G10 and flow cytometry. Chemotaxis assays were performed as described earlier, with chemotaxis stimulated by 30 nM CXCL12.

### Electroporation of Jurkat cells

Jurkat cells ($1 \times 10^6$) were centrifuged and resuspended in 100 ml Cell Line Nucleofector Solution V (Lonza) containing 300 nM Silencer Select BA1- and BA2-specific siRNA (Thermo Fisher Scientific). The suspension of cells and RNA was transferred to an electroporation cuvette (Lonza) and subjected to the Nucleofector Program X-005 electroporation program using an Amaxa electroporator device. Cells were incubated in the cuvette for 10 min before being transferred into culture medium consisting of RPMI 1640 (Sigma-Aldrich) supplemented with 10% heat-inactivated FBS (Sigma-Aldrich), 1% penicillin-streptomycin (Thermo Fisher Scientific), and a final concentration of 2 μM L-glutamine (Thermo Fisher Scientific). Cells were left for 24 hours before being analyzed for ERK1/2 phosphorylation.

### Endocytosis assay

Jurkat cells ($1 \times 10^5$) were serum-starved for 6 hours and incubated with vehicle or CXCR4 antagonist 30 min before stimulation with 30 nM CXCL12. After the designated time, cells were washed three times in ice-cold PBS containing 1% BSA, before incubation with the PE-tagged CXCR4 monoclonal antibody 4G10 or 12G5, or suitable isotype controls for 20 min. Cells were washed twice in PBS before being fixed in PBS containing 4% paraformaldehyde. Cell surface expression of CXCR4 was determined by flow cytometry using a Beckman Coulter flow cytometer, and data were analyzed by WinMDI software.

### ERK1/2 phosphorylation assay

Cells ($1 \times 10^7$) were serum-starved for 6 hours before the start of the assay. After starvation, the cells were treated with vehicle (PBS) or 30 nM CXCL12 for several time points up to 30 min. Cells were harvested, washed three times in ice-cold PBS, and lysed in RIPA buffer for analysis by SDS-PAGE and Western blotting.

### Fluorescence spectroscopy

Fluorescence measurements were performed on a PTI Quantamaster instrument. CXCL12 or a mixture of X4-2-6 and CXCL12 was analyzed at 25°C. The emission profile was scanned from 300 to 420 nm when the excitation was set to 280 nm. The concentration of X4-2-6 nanoparticles and CXCL12 was maintained at 1 and 0.083 μM, respectively, for all measurements.

### Western blotting

To detect changes in cell signaling, cells were lysed in ice-cold RIPA buffer (10μM tris-HCl, 140 nM NaCl, 1 μM EDTA, 1% Triton X-100, 0.1 % sodium deoxycholate, and 0.1% SDS) containing protease cocktail inhibitor (Santa Cruz Biotechnology) and phosphatase inhibitors (10 mM NaF and 1 mM $Na_3OV_4$). Cells were lysed by sonication, cell debris was pelleted by centrifugation, and the supernatant was collected. Total protein concentrations were measured. Samples were mixed with SDS-PAGE sample buffer and boiled at 90°C for 3 min. Proteins were resolved by SDS-PAGE and transferred onto nitrocellulose membranes for detection with the appropriate antibodies. All Western blots in the figures are representative of at least three independent experiments.

### Immunoprecipitation

To detect changes in GTP loading of Gαi, $1 \times 10^7$ Jurkat cells were serum-starved for 6 hours and then treated as indicated in the figure legends. Cells were lysed by sonication in ice-cold immunoprecipitation lysis buffer [20 mM tris-HCl (pH 8.0), 140 nM NaCl, and 2 mM EDTA] containing protease cocktail inhibitor (Santa Cruz Biotechnology) and phosphatase inhibitors (10 mM NaF and 1 mM $Na_3OV_4$), cell debris was pelleted, and the supernatant was collected. Cell lysates were incubated with the antiactive Gαi antibody overnight at 4°C, before addition of 5 μl of protein A Dynabeads (Thermo Fisher Scientific) for 1 hour at room temperature. Immunoprecipitated proteins were eluted from the beads using SDS-PAGE loading buffer lacking dithiothreitol [50 mM tris-HCl (pH 6.8), 2% SDS, 0.1% bromophenol blue, 10% glycerol].

### NMR spectroscopy

$^{1}H$-$^{15}N$ HSQC experiments were performed on 50 μM recombinant human CXCL12 (Protein Foundry) and dissolved in PBS (pH 7.4) containing 10% $D_2O$. Experiments were performed in the presence and absence of 10 μM X4-2-6, 1 μM AMD3100, and 10-mg membranes from WT CHO-K1 cells or CHO-K1 cells expressing CXCR4. All NMR experiments were performed on a 900-MHz Bruker Avance spectrometer equipped with a cryogenic probe. Data processing and analysis were performed with NMRPipe software (70). The chemical shift assignments were taken from the Biological Magnetic Resonance Data Bank (BMRB) database (www.bmrb.wisc.edu) using the 16142 BMRB identification number. Changes in signal intensity were calculated by subtracting the signal intensity of experimental spectra ($I$) from control spectra ($I_0$) divided by $I_0$ and plotted as a ratio. Mean chemical shift difference was calculated as follows

$$\Delta\delta_{NH} = \sqrt{\frac{\left(\Delta\delta^{1}H\right)^{2} + \left(\Delta\delta^{15}N\right)^{2}/25}{2}}$$

Changes in signal intensity and chemical shift perturbations higher than the sum of the average and 1 SD were considered statistically significant.

### Preparation of cell membrane fractions

Jurkat cells ($1 \times 10^7$) were collected and washed three times with PBS before lysis by sonication in 1 ml of fractionation buffer [250 mM sucrose, 20 mM Hepes (pH 7.4), 10 mM KCl, 2 mM $MgCl_2$, 1 mM EDTA, 1 mM EGTA, protease cocktail inhibitor (Santa Cruz Biotechnology), 10 mM NaF, and 1 mM $Na_3OV_4$]. Samples were then centrifuged at 10,000$g$ for 10 min, and the supernatant was transferred to a fresh ultracentrifuge tube. The sample was spun in a Beckman L8–80M centrifuge at 100,000$g$ for 1 hour at 4°C. The subsequent pellet was washed once in 500 ml of fractionation buffer before being resuspended in sterile PBS.

### PRESTO-Tango Assay

BA2 recruitment to CXCR4 was measured by the PRESTO-Tango assay, as previously described (37). Briefly, HTLA cells were transfected with Tango plasmids (both provided by B. Roth) using Lipofectamine 3000 (Thermo Fisher Scientific). One day after transfection, HTLA cells were plated onto poly-L-Lysine precoated 96-well microplates and allowed to attach to the platefor 4 hours before treatment. Cells were treated with increasing concentrations of CXCL12 in the presence of vehicle, 1 μM AMD3100, or 10 μM X4-2-6 for 1 hour at 37°C, 5% $CO_2$ in a humidified environment. Cells were then incubated with culture medium with 100 ml of a 1:5 mixture of Bright-Glo (Promega) and 1× HBSS and 20 mM Hepes solution. Plates were incubated at room temperature before measuring luminescence on a BioTek Synergy 2 plate reader.

### Prolonged exposure to CXCR4 antagonists

In culture medium, $1 \times 10^7$ Jurkat cells were exposed to the concentrations of CXCR4 antagonists indicated in the figure legends. At 12-hour intervals, cells were pelleted by

centrifugation, washed three times with PBS, and resuspended in fresh culture medium containing CXCR4 antagonists. After 72 hours, cells were counted using a hemocytometer and prepared for subsequent assays.

### Protein sequence alignment

Amino acid sequences of proteins were acquired from the UniProt website, and alignments were performed using the MultAlin website and the ESPript 3.0 ENDscript server (71).

### Statistical analysis

Quantification of band densities from Western blots was performed with ImageJ software (72). At any data point, P values were determined by the statistical tests defined in the figure legends, with post hoc analysis where appropriate.

## Supplementary Material

Refer to Web version on PubMed Central for supplementary material.

## Acknowledgments:

We thank B. Roth (School of Medicine at the University of North Carolina at Chapel Hill) for sharing the PRESTO-Tango plasmids.

**Funding:** This work was funded by the National Institutes of Health (NIH)–National Cancer Institute (NCI) R01CA188427 grant to V.G., NIH-NIGMS R01GM107495 to M.M., and NIH-NIAID R01AI058072 to B.F.V.

## REFERENCES AND NOTES

1. Fredriksson R, Lagerstrom MC, Lundin L-G, Schiöth HB, The G-protein-coupled receptors in the human genome form five main families. Phylogenetic analysis, paralogon groups, and fingerprints. Mol. Pharmacol 63, 1256–1272 (2003). [PubMed: 12761335]
2. International Human Genome Sequencing Consortium, Initial sequencing and analysis of the human genome. Nature 409, 860–921 (2001). [PubMed: 11237011]
3. Venter JC, Adams MD, Myers EW, Li PW, Mural RJ, Sutton GG, Smith HO,Yandell M, Evans CA, Holt RA, Gocayne JD, Amanatides P, Ballew RM, Huson DH,Wortman JR, Zhang Q, Kodira CD, Zheng XH, Chen L, Skupski M, Subramanian G,Thomas PD, Zhang J, Gabor Miklos GL, Nelson C, Broder S, Clark AG, Nadeau J,McKusick VA, Zinder N, Levine AJ, Roberts RJ, Simon M, Slayman C, Hunkapiller M,Bolanos R, Delcher A, Dew I, Fasulo D, Flanigan M, Florea L, Halpern A, Hannenhalli S,Kravitz S, Levy S, Mobarry C, Reinert K, Remington K, Abu-Threideh J, Beasley E,Biddick K, Bonazzi V, Brandon R, Cargill M, Chandramouliswaran I, Charlab R,Chaturvedi K, Deng Z, Di Francesco V, Dunn P, Eilbeck K, Evangelista C, Gabrielian AE,Gan W, Ge W, Gong F, Gu Z, Guan P, Heiman TJ, Higgins ME, Ji RR, Ke Z,Ketchum KA, Lai Z, Lei Y, Li Z, Li J, Liang Y, Lin X, Lu F, Merkulov GV, Milshina N,Moore HM, Naik AK, Narayan VA, Neelam B, Nusskern D, Rusch DB, Salzberg S,Shao W, Shue B, Sun J, Wang Z, Wang A, Wang X, Wang J, Wei M, Wides R,Xiao C, Yan C, Yao A, Ye J, Zhan M, Zhang W, Zhang H, Zhao Q, Zheng L, Zhong F,Zhong W, Zhu S, Zhao S, Gilbert D, Baumhueter S, Spier G, Carter C, Cravchik A,Woodage T, Ali F, An H, Awe A, Baldwin D, Baden H, Barnstead M, Barrow I, Beeson K,Busam D, Carver A, Center A, Cheng ML, Curry L, Danaher S, Davenport L, Desilets R,Dietz S, Dodson K, Doup L, Ferriera S, Garg N, Gluecksmann A, Hart B, Haynes J,Haynes C, Heiner C, Hladun S, Hostin D, Houck J, Howland T, Ibegwam C, Johnson J,Kalush F, Kline L, Koduru S, Love A, Mann F, May D, McCawley S, McIntosh T,McMullen I, Moy M, Moy L, Murphy B, Nelson K, Pfannkoch C, Pratts E, Puri V,Qureshi H, Reardon M, Rodriguez R, Rogers YH, Romblad D, Ruhfel B, Scott R, Sitter C,Smallwood M, Stewart E, Strong R, Suh E, Thomas R, Tint NN, Tse S, Vech C,Wang G, Wetter J, Williams S, Williams M, Windsor S, Winn-Deen E, Wolfe K, Zaveri J,Zaveri K, Abril JF, Guigo R,

Campbell MJ, Sjolander KV, Karlak B, Kejariwal A,Mi H, Lazareva B, Hatton T, Narechania A, Diemer K, Muruganujan A, Guo N, Sato S,Bafna V, Istrail S, Lippert R, Schwartz R, Walenz B, Yooseph S, Allen D, Basu A,Baxendale J, Blick L, Caminha M, Carnes-Stine J, Caulk P, Chiang YH, Coyne M,Dahlke C, Mays A, Dombroski M, Donnelly M, Ely D, Esparham S, Fosler C, Gire H,Glanowski S, Glasser K, Glodek A, Gorokhov M, Graham K, Gropman B, Harris M, Heil J,Henderson S, Hoover J, Jennings D, Jordan C, Jordan J, Kasha J, Kagan L, Kraft C,Levitsky A, Lewis M, Liu X, Lopez J, Ma D, Majoros W, McDaniel J, Murphy S,Newman M, Nguyen T, Nguyen N, Nodell M, Pan S, Peck J, Peterson M, Rowe W,Sanders R, Scott J, Simpson M, Smith T, Sprague A, Stockwell T, Turner R,Venter E, Wang M, Wen M, Wu D, Wu M, Xia A, Zandieh A, Zhu X, The sequence of the human genome. Science 291, 1304–1351 (2001). [PubMed: 11181995]

4. Sriram K, Insel PA, G protein-coupled receptors as targets for approved drugs: How many targets and how many drugs? Mol. Pharmacol 93, 251–258 (2018). [PubMed: 29298813]
5. Allouche S, Noble F, Marie N, Opioid receptor desensitization: Mechanisms and its link to tolerance. Front. Pharmacol 5, 280 (2014). [PubMed: 25566076]
6. Gomes BA, Shen J, Stafford K, Patel M, Yoburn BC, m-opioid receptor down-regulation and tolerance are not equally dependent upon G-protein signaling. Pharmacol. Biochem. Behav 72, 273–278 (2002). [PubMed: 11900797]
7. Silvestri S, Seeman MV, Negrete JC, Houle S, Shammi CM, Remington GJ, Kapur S,Zipursky RB, Wilson AA, Christensen BK, Seeman P, Increased dopamine D2 receptor binding after long-term treatment with antipsychotics in humans: A clinical PET study. Psychopharmacology 152, 174–180 (2000). [PubMed: 11057521]
8. Vincent J, Dachman W, Blaschke TF, Hoffman BB, Pharmacological tolerance to alpha 1-adrenergic receptor antagonism mediated by terazosin in humans. J. Clin. Invest 90, 1763–1768 (1992). [PubMed: 1358918]
9. Zhang L, Taniguchi T, Tanaka T, Shinozuka K, Kunitomo M, Nishiyama M, Kamata K,Muramatsu I, Alpha-1 adrenoceptor up-regulation induced by prazosin but not KMD-3213 or reserpine in rats. Br. J. Pharmacol 135, 1757–1764 (2002). [PubMed: 11934817]
10. Ohkuma S, Katsura M, Shibasaki M, Tsujimura A, Hirouchi M, Expression of β-adrenergic receptor up-regulation is mediated by two different processes. Brain Res 1112, 114–125 (2006). [PubMed: 16920085]
11. Sison EAR, Magoon D, Li L, Annesley CE, Rau RE, Small D, Brown P, Plerixafor as a chemosensitizing agent in pediatric acute lymphoblastic leukemia: Efficacy and potential mechanisms of resistance to CXCR4 inhibition. Oncotarget 5, 8947–8958 (2014). [PubMed: 25333254]
12. McGrath KE, Koniski AD, Maltby KM, McGann JK, Palis J, Embryonic expression and function of the chemokine SDF-1 and its receptor, CXCR4. Dev. Biol 213, 442–456 (1999). [PubMed: 10479460]
13. Dar A, Kollet O, Lapidot T, Mutual, reciprocal SDF-1/CXCR4 interactions between hematopoietic and bone marrow stromal cells regulate human stem cell migration and development in NOD/SCID chimeric mice. Exp. Hematol 34, 967–975 (2006). [PubMed: 16863903]
14. Möhle R, Bautz F, Rafii S, Moore MAS, Brugger W, Kanz L, The chemokine receptor CXCR-4 is expressed on $CD34^+$ hematopoietic progenitors and leukemic cells and mediates transendothelial migration induced by stromal cell-derived factor-1. Blood 91, 4523–4530 (1998). [PubMed: 9616148]
15. Ponomaryov T, Peled A, Petit I, Taichman RS, Habler L, Sandbank J, Arenzana-Seisdedos F,Magerus A, Caruz A, Fujii N, Nagler A, Lahav M, Szyper-Kravitz M, Zipori D, Lapidot T, Induction of the chemokine stromal-derived factor-1 following DNA damage improves human stem cell function. J. Clin. Invest 106, 1331–1339 (2000). [PubMed: 11104786]
16. Sugiyama T, Kohara H, Noda M, Nagasawa T, Maintenance of the hematopoietic stem cell pool by CXCL12-CXCR4 chemokine signaling in bone marrow stromal cell niches. Immunity 25, 977–988 (2006). [PubMed: 17174120]
17. Doranz BJ, Orsini MJ, Turner JD, Hoffman TL, Berson JF, Hoxie JA, Peiper SC,Brass LF, Doms RW, Identification of CXCR4 domains that support coreceptor and chemokine receptor functions. J. Virol 73, 2752–2761 (1999). [PubMed: 10074122]

18. Onai N, Zhang Y, Yoneyama H, Kitamura T, Ishikawa S, Matsushima K, Impairment of lymphopoiesis and myelopoiesis in mice reconstituted with bone marrow-hematopoietic progenitor cells expressing SDF-1-intrakine. Blood 96, 2074–2080 (2000). [PubMed: 10979950]
19. Chatterjee S, Behnam Azad B, Nimmagadda S, The intricate role of CXCR4 in cancer. Adv. Cancer Res 124, 31–82 (2014). [PubMed: 25287686]
20. National Cancer Institute (2013); www.cancer.gov/about-cancer/treatment/drugs/plerixafor.
21. Uy GL, Rettig MP, Motabi IH, McFarland K, Trinkaus KM, Hladnik LM, Kulkarni S,Abboud CN, Cashen AF, Stockerl-Goldstein KE, Vij R, Westervelt P, DiPersio JF, A phase 1/2 study of chemosensitization with the CXCR4 antagonist plerixafor in relapsed or refractory acute myeloid leukemia. Blood 119, 3917–3924 (2012). [PubMed: 22308295]
22. Hatse S, Princen K, Bridger G, De Clercq E, Schols D, Chemokine receptor inhibition by AMD3100 is strictly confined to CXCR4. FEBS Lett 527, 255–262 (2002). [PubMed: 12220670]
23. Orsini MJ, Parent J-L, Mundell SJ, Marchese A, Benovic JL, Trafficking of the HIV coreceptor CXCR4. Role of arrestins and identification of residues in the c-terminal tail that mediate receptor internalization. J. Biol. Chem 274, 31076–31086 (1999). [PubMed: 10521508]
24. Castaldo C, Benicchi T, Otrocka M, Mori E, Pilli E, Ferruzzi P, Valensin S, Diamanti D,Fecke W, Varrone M, Porcari V, CXCR4 antagonists: A screening strategy for identification of functionally selective ligands. J. Biomol. Screen 19, 859–869 (2014). [PubMed: 24632660]
25. Gilchrist A, Gauntner TD, Fazzini A, Alley KM, Pyen DS, Ahn J, Ha SJ, Willett A,Sansom SE, Yarfi JL, Bachovchin KA, Mazzoni MR, Merritt JR, Identifying bias in CCR1 antagonists using radiolabelled binding, receptor internalization, β-arrestin translocation and chemotaxis assays. Br. J. Pharmacol 171, 5127–5138 (2014). [PubMed: 24990525]
26. Magnan R, Escrieut C, Gigoux V, De K, Clerc P, Niu F, Azema J, Masri B, Cordomi A,Baltas M, Tikhonova IG, Fourmy D, Distinct CCK-2 receptor conformations associated with b-arrestin-2 recruitment or phospholipase-C activation revealed by a biased antagonist. J. Am. Chem. Soc 135, 2560–2573 (2013). [PubMed: 23323542]
27. Ramachandran R, Noorbakhsh F, Defea K, Hollenberg MD, Targeting proteinase-activated receptors: Therapeutic potential and challenges. Nat. Rev. Drug Discov 11, 69–86 (2012). [PubMed: 22212680]
28. Delgado MB, Clark-Lewis I, Loetscher P, Langen H, Thelen M, Baggiolini M, Wolf M, Rapid inactivation of stromal cell-derived factor-1 by cathepsin G associated with lymphocytes. Eur. J. Immunol 31, 699–707 (2001). [PubMed: 11241273]
29. Kofuku Y, Yoshiura C, Ueda T, Terasawa H, Hirai T, Tominaga S, Hirose M, Maeda Y,Takahashi H, Terashima Y, Matsushima K, Shimada I, Structural basis of the interaction between chemokine stromal cell-derived factor-1/CXCL12 and its G-protein-coupled receptor CXCR4. J. Biol. Chem 284, 35240–35250 (2009). [PubMed: 19837984]
30. Kufareva I, Stephens BS, Holden LG, Qin L, Zhao C, Kawamura T, Abagyan R,Handel TM, Stoichiometry and geometry of the CXC chemokine receptor 4 complex with CXC ligand 12: Molecular modeling and experimental validation. Proc. Natl. Acad. Sci. U.S.A 111, E5363–E5372 (2014). [PubMed: 25468967]
31. Qin L, Kufareva I, Holden LG, Wang C, Zheng Y, Zhao C, Fenalti G, Wu H, Han GW,Cherezov V, Abagyan R, Stevens RC, Handel TM, Structural biology. Crystal structure of the chemokine receptor CXCR4 in complex with a viral chemokine. Science 347, 1117–1122 (2015). [PubMed: 25612609]
32. Tamamis P, Floudas CA, Elucidating a key component of cancer metastasis: CXCL12 (SDF-1alpha) binding to CXCR4. J. Chem. Inf. Model 54, 1174–1188 (2014). [PubMed: 24660779]
33. Tarasov SG, Gaponenko V, Howard OM, Chen Y, Oppenheim JJ, Dyba MA,Subramaniam S, Lee Y, Michejda C, Tarasova NI, Structural plasticity of a transmembrane peptide allows self-assembly into biologically active nanoparticles. Proc. Natl. Acad. Sci. U.S.A 108, 9798–9803 (2011). [PubMed: 21628584]
34. Smith MCP, Luker KE, Garbow JR, Prior JL, Jackson E, Piwnica-Worms D,Luker GD, CXCR4 regulates growth of both primary and metastatic breast cancer. Cancer Res 64, 8604–8612 (2004). [PubMed: 15574767]

35. Follesa P, Ticku MK, NMDA receptor upregulation: Molecular studies in cultured mouse cortical neurons after chronic antagonist exposure. J. Neurosci 16, 2172–2178 (1996). [PubMed: 8601798]
36. Kang DS, Tian X, Benovic JL, Role of b-arrestins and arrestin domain-containing proteins in G protein-coupled receptor trafficking. Curr. Opin. Cell Biol 27, 63–71 (2014). [PubMed: 24680432]
37. Kroeze WK, Sassano MF, Huang X-P, Lansu K, McCorvy JD, Giguere PM, Sciaky N,Roth BL, PRESTO-Tango as an open-source resource for interrogation of the druggable human GPCRome. Nat. Struct. Mol. Biol 22, 362–369 (2015). [PubMed: 25895059]
38. Marchese A, Trejo J, Ubiquitin-dependent regulation of G protein-coupled receptor trafficking and signaling. Cell. Signal 25, 707–716 (2013). [PubMed: 23201781]
39. Tarasova NI, Rice WG, Michejda CJ, Inhibition of G-protein-coupled receptor function by disruption of transmembrane domain interactions. J. Biol. Chem 274, 34911–34915 (1999). [PubMed: 10574965]
40. Percherancier Y, Berchiche YA, Slight I, Volkmer-Engert R, Tamamura H, Fujii N,Bouvier M, Heveker N, Bioluminescence resonance energy transfer reveals ligand-induced conformational changes in CXCR4 homo- and heterodimers. J. Biol. Chem 280, 9895–9903 (2005). [PubMed: 15632118]
41. Ahn S, Shenoy SK, Wei H, Lefkowitz RJ, Differential kinetic and spatial patterns of beta-arrestin and G protein-mediated ERK activation by the angiotensin II receptor.J. Biol. Chem 279, 35518–35525 (2004). [PubMed: 15205453]
42. Cheng Z-J, Zhao J, Sun Y, Hu W, Wu Y-L, Cen B, Wu G-X, Pei G, β-arrestin differentially regulates the chemokine receptor CXCR4-mediated signaling and receptor internalization, and this implicates multiple interaction sites between b-arrestin and CXCR4. J. Biol. Chem 275, 2479–2485 (2000). [PubMed: 10644702]
43. Quoyer J, Janz JM, Luo J, Ren Y, Armando S, Lukashova V, Benovic JL, Carlson KE,Hunt SW, III, Bouvier M, Pepducin targeting the C-X-C chemokine receptor type 4 acts as a biased agonist favoring activation of the inhibitory G protein. Proc. Natl. Acad. Sci. U.S.A 110, E5088–E5097 (2013). [PubMed: 24309376]
44. Malik R, Soh UJK, Trejo J, Marchese A, Novel roles for the E3 ubiquitin ligase atrophin-interacting protein 4 and signal transduction adaptor molecule 1 in G protein-coupled receptor signaling. J. Biol. Chem 287, 9013–9027 (2012). [PubMed: 22275353]
45. Beautrait A, Paradis JS, Zimmerman B, Giubilaro J, Nikolajev L, Armando S, Kobayashi H,Yamani L, Namkung Y, Heydenreich FM, Khoury E, Audet M, Roux PP, Veprintsev DB,Laporte SA, Bouvier M, A new inhibitor of the β-arrestin/AP2 endocytic complex reveals interplay between GPCR internalization and signalling. Nat. Commun 8, 15054 (2017). [PubMed: 28416805]
46. Kohout TA, Lin FS, Perry SJ, Conner DA, Lefkowitz RJ, β-Arrestin 1 and 2 differentially regulate heptahelical receptor signaling and trafficking. Proc. Natl. Acad. Sci. U.S.A 98, 1601–1606 (2001). [PubMed: 11171997]
47. Seamon KB, Padgett W, Daly JW, Forskolin: Unique diterpene activator of adenylate cyclase in membranes and in intact cells. Proc. Natl. Acad. Sci. U.S.A 78, 3363–3367 (1981). [PubMed: 6267587]
48. Ikeda SR, Voltage-dependent modulation of N-type calcium channels by G-protein β γsubunits. Nature 380, 255–258 (1996). [PubMed: 8637575]
49. Veldkamp CT, Ziarek JJ, Su J, Basnet H, Lennertz R, Weiner JJ, Peterson FC,Baker JE, Volkman BF, Monomeric structure of the cardioprotective chemokine SDF-1/CXCL12. Protein Sci 18, 1359–1369 (2009). [PubMed: 19551879]
50. Wu B, Chien EYT, Mol CD, Fenalti G, Liu W, Katritch V, Abagyan R, Brooun A,Wells P, Bi FC, Hamel DJ, Kuhn P, Handel TM, Cherezov V, Stevens RC, Structures of the CXCR4 chemokine GPCR with small-molecule and cyclic peptide antagonists. Science 330, 1066–1071 (2010). [PubMed: 20929726]
51. Veldkamp CT, Seibert C, Peterson FC, De la Cruz NB, Haugner JC, III, Basnet H,Sakmar TP, Volkman BF, Structural basis of CXCR4 sulfotyrosine recognition by the chemokine SDF-1/CXCL12. Sci. Signal 1, ra4 (2008). [PubMed: 18799424]

52. Crump MP, Gong JH, Loetscher P, Rajarathnam K, Amara A, Arenzana-Seisdedos F,Virelizier JL, Baggiolini M, Sykes BD, Clark-Lewis I, Solution structure and basis for functional activity of stromal cell-derived factor-1; dissociation of CXCR4 activation from binding and inhibition of HIV-1. EMBO J 16, 6996–7007 (1997). [PubMed: 9384579]
53. Aarons RD, Nies AS, Gal J, Hegstrand LR, Molinoff PB, Elevation of beta-adrenergic receptor density in human lymphocytes after propranolol administration. J. Clin. Invest 65, 949–957 (1980). [PubMed: 6102572]
54. Signoret N, Oldridge J, Pelchen-Matthews A, Klasse PJ, Tran T, Brass LF,Rosenkilde MM, Schwartz TW, Holmes W, Dallas W, Luther MA, Wells TNC,Hoxie JA, Marsh M, Phorbol esters and SDF-1 induce rapid endocytosis and down modulation of the chemokine receptor CXCR4. J. Cell Biol 139, 651–664 (1997). [PubMed: 9348282]
55. Busillo JM, Armando S, Sengupta R, Meucci O, Bouvier M, Benovic JL, Site-specific phosphorylation of CXCR4 is dynamically regulated by multiple kinases and results in differential modulation of CXCR4 signaling. J. Biol. Chem 285, 7805–7817 (2010). [PubMed: 20048153]
56. Grundler R, Brault L, Gasser C, Bullock AN, Dechow T, Woetzel S, Pogacic V, Villa A,Ehret S, Berridge G, Spoo A, Dierks C, Biondi A, Knapp S, Duyster J, Schwaller J, Dissection of PIM serine/threonine kinases in FLT3-ITD–induced leukemogenesis reveals PIM1 as regulator of CXCL12–CXCR4-mediated homing and migration. J. Exp. Med 206, 1957–1970 (2009). [PubMed: 19687226]
57. Elorza A, Penela P, Sarnago S, Mayor F, Jr., MAPK-dependent degradation of G protein-coupled receptor kinase 2. J. Biol. Chem 278, 29164–29173 (2003). [PubMed: 12738776]
58. Loudon RP, Perussia B, Benovic JL, Differentially regulated expression of the G-protein-coupled receptor kinases, betaARK and GRK6, during myelomonocytic cell development in vitro. Blood 88, 4547–4557 (1996). [PubMed: 8977246]
59. Luo Y, Lathia J, Mughal M, Mattson MP, SDF1a/CXCR4 signaling, via ERKs and the transcription factor Egr1, induces expression of a 67-kDa form of glutamic acid decarboxylase in embryonic hippocampal neurons. J. Biol. Chem 283, 24789–24800 (2008). [PubMed: 18606818]
60. Kremer KN, Clift IC, Miamen AG, Bamidele AO, Qian N-X, Humphreys TD,Hedin KE, Stromal cell-derived factor-1 signaling via the CXCR4-TCR heterodimer requires phospholipase C-β3 and phospholipase C-γ1 for distinct cellular responses. J. Immunol 187, 1440–1447 (2011). [PubMed: 21705626]
61. Lefkowitz RJ, Shenoy SK, Transduction of receptor signals by b-arrestins. Science 308, 512–517 (2005). [PubMed: 15845844]
62. Tohgo A, Pierce KL, Choy EW, Lefkowitz RJ, Luttrell LM, β-arrestin scaffolding of the ERK cascade enhances cytosolic ERK activity but inhibits ERK-mediated transcription following angiotensin AT1a receptor stimulation. J. Biol. Chem 277, 9429–9436 (2002). [PubMed: 11777902]
63. Luo J, Busillo JM, Benovic JL, $M_3$ muscarinic acetylcholine receptor-mediated signaling is regulated by distinct mechanisms. Mol. Pharmacol 74, 338–347 (2008). [PubMed: 18388243]
64. Jung S-R, Kushmerick C, Seo JB, Koh D-S, Hille B, Muscarinic receptor regulates extracellular signal regulated kinase by two modes of arrestin binding. Proc. Natl. Acad. Sci. U.S.A 114, E5579–E5588 (2017). [PubMed: 28652372]
65. Zhao M, Wimmer A, Trieu K, DiScipio RG, Schraufstatter IU, Arrestin regulates MAPK activation and prevents NADPH oxidase-dependent death of cells expressing CXCR2.J. Biol. Chem 279, 49259–49267 (2004). [PubMed: 15364949]
66. Grundmann M, Merten N, Malfacini D, Inoue A, Preis P, Simon K, Rüttiger N, Ziegler N,Benkel T, Schmitt NK, Ishida S, Müller I, Reher R, Kawakami K, Inoue A, Rick U, Kühl T,Imhof D, Aoki J, König GM, Hoffmann C, Gomeza J, Wess J, Kostenis E, Lack of beta-arrestin signaling in the absence of active G proteins. Nat. Commun 9, 341 (2018). [PubMed: 29362459]
67. Liebick M, Henze S, Vogt V, Oppermann M, Functional consequences of chemically-induced β-arrestin binding to chemokine receptors CXCR4 and CCR5 in the absence of ligand stimulation. Cell. Signal 38, 201–211 (2017). [PubMed: 28733085]
68. Zhang W.-b., Navenot J-M, Haribabu B, Tamamura H, Hiramatu K, Omagari A, Pei G, Manfredi JP, Fujii N, Broach JR, Peiper SC, A point mutation that confers constitutive activity to CXCR4

reveals that T140 is an inverse agonist and that AMD3100 and ALX40–4C are weak partial agonists. J. Biol. Chem 277, 24515–24521 (2002). [PubMed: 11923301]

69. O'Reilly LA, Kruse EA, Puthalakath H, Kelly PN, Kaufmann T, Huang DCS,Strasser A, MEK/ERK-mediated phosphorylation of Bim is required to ensure survival of T and B lymphocytes during mitogenic stimulation. J. Immunol 183, 261–269 (2009). [PubMed: 19542438]
70. Delaglio F, Grzesiek S, Vuister GW, Zhu G, Pfeifer J, Bax A, NMRPipe: A multidimensional spectral processing system based on UNIX pipes. J. Biomol. NMR 6, 277–293 (1995). [PubMed: 8520220]
71. Robert X, Gouet P, Deciphering key features in protein structures with the new ENDscript server. Nucleic Acids Res. 42, W320–W324 (2014). [PubMed: 24753421]
72. Schneider CA, Rasband WS, Eliceiri KW, NIH Image to ImageJ: 25 years of image analysis. Nat. Methods 9, 671–675 (2012). [PubMed: 22930834]

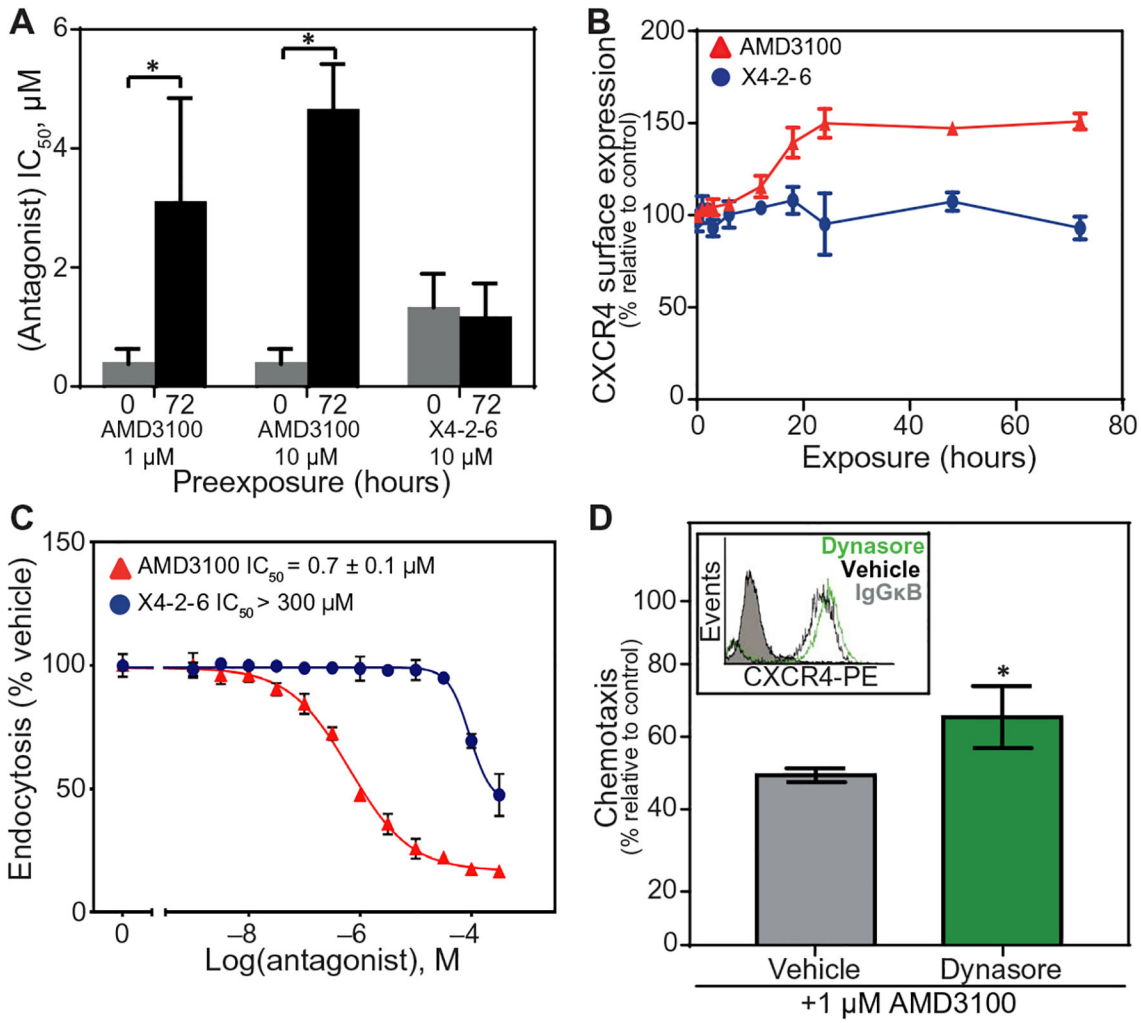


**Fig. 1. Antagonist tolerance develops after inhibition of endocytosis.**

**(A)** $IC_{50}$ values calculated from Transwell chemotaxis assays of Jurkat cell migration toward CXCL12 after pre-treatment with AMD3100 or X4-2-6 at the indicated concentrations for the indicated times. Data are means ± SEM of three independent experiments. *$P < 0.001$ by Student's *t* test. (**B**) Flow cytometry analysis of CXCR4 cell surface expression on Jurkat cells treated with AMD3100 (▲) or X4-2-6 (●) for 72 hours as compared to vehicle-treated cells. Data are means ± SD of three experiments performed in triplicate at each condition. (**C**) Flow cytometry analysis of CXCR4 endocytosis stimulated by CXCL12 in Jurkat cells treated with AMD3100 (▲) or X4-2-6 (●) as compared to cells stimulated with CXCL12 alone. Data are means ± SD from three experiments performed in triplicate for each condition. (**D**) Transwell migration assay of Jurkat cell chemotaxis toward CXCL12 after treatment with the indicated concentration of AMD3100 with or without dynasore for 1 hour. Chemotaxis is plotted relative to chemotaxis in the presence of CXCL12 alone. Data are means ± SD from three independent experiments performed in triplicate for each condition. *$P < 0.04$ by Student's t test. Flow cytometry analysis of CXCR4 cell surface

expression before and after dynasore treatment (upper left inset) is representative of all experiments. IgGκB, immunoglobulin G κB; PE, phycoerythrin.

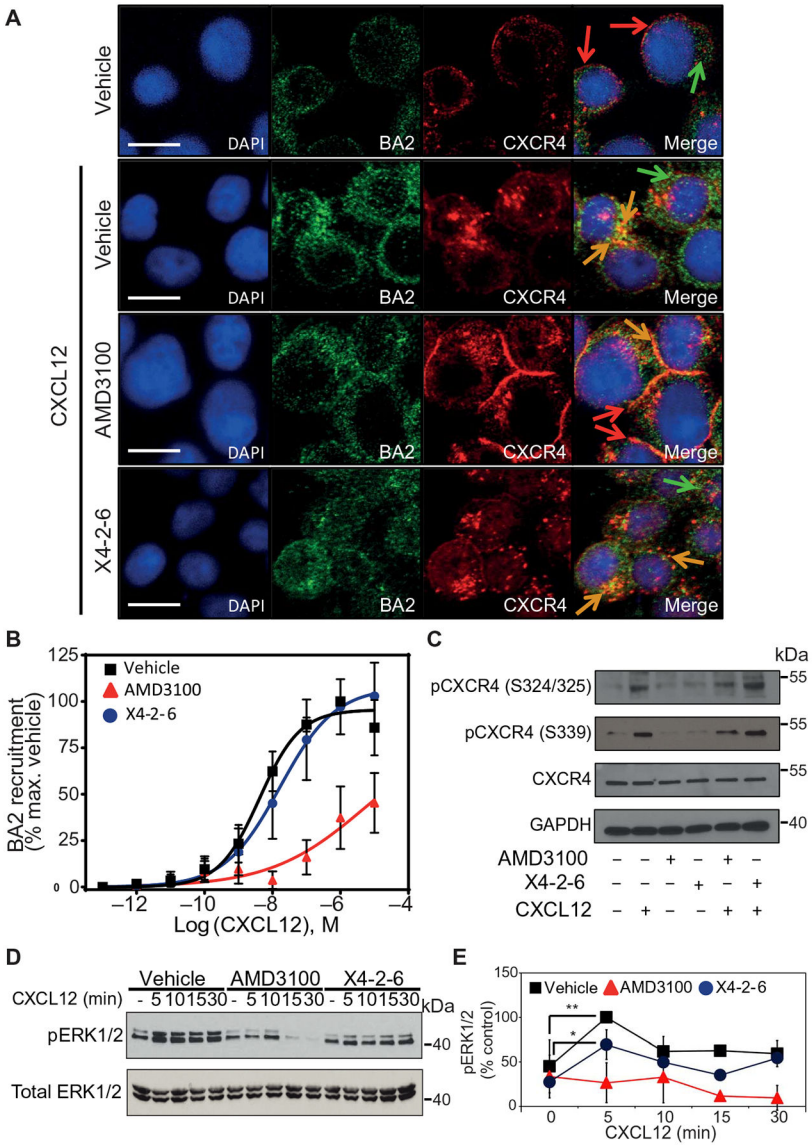


**Fig. 2. BA1/2 recruitment and function downstream of CXCR4 is not substantially affected by X4-2-6.**

**(A)** Confocal microscopy analysis of CXCR4 and BA2 in Jurkat cells pretreated with vehicle, AMD3100, or X4-2-6 and stimulated with CXCL12, as indicated. Arrows indicate CXCR4 (red), BA2 (green), or colocalization (orange). Images are representative of three independent experiments. Scale bars, 10 μM. DAPI, 4′,6-diamidino-2-phenylindole, dihydrochloride. (**B**) PRESTO-Tango assay analysis of the recruitment of BA1/2 to CXCR4 after treatment with increasing concentrations of CXCL12 in the presence of vehicle (■), AMD3100 (▲), or X4-2-6 (●). Data are means ± SD of three independent experiments performed on six replicates per condition. (**C**) Western blotting analysis of CXCR4 $Ser^{324/325}$ and $Ser^{339}$ phosphorylation in lysates of Jurkat cells treated as indicated. Blots are representative of at least three independent experiments. GAPDH, glyceraldehyde-3-phosphate dehydrogenase. (**D** and **E**) Western blotting analysis of ERK1/2 $Thr^{202}/Tyr^{204}$ phosphorylation in the lysates of Jurkat cells treated as indicated. (D) Blots are

representative of at least three independent experiments. (E) Quantification of the relative abundance of pERK1/2 normalized to that of total ERK1/2. Data are means ± SD from all experiments. *$P < 0.05$ and **$P < 0.01$ by one-way analysis of variance (ANOVA) with post hoc Tukey test.

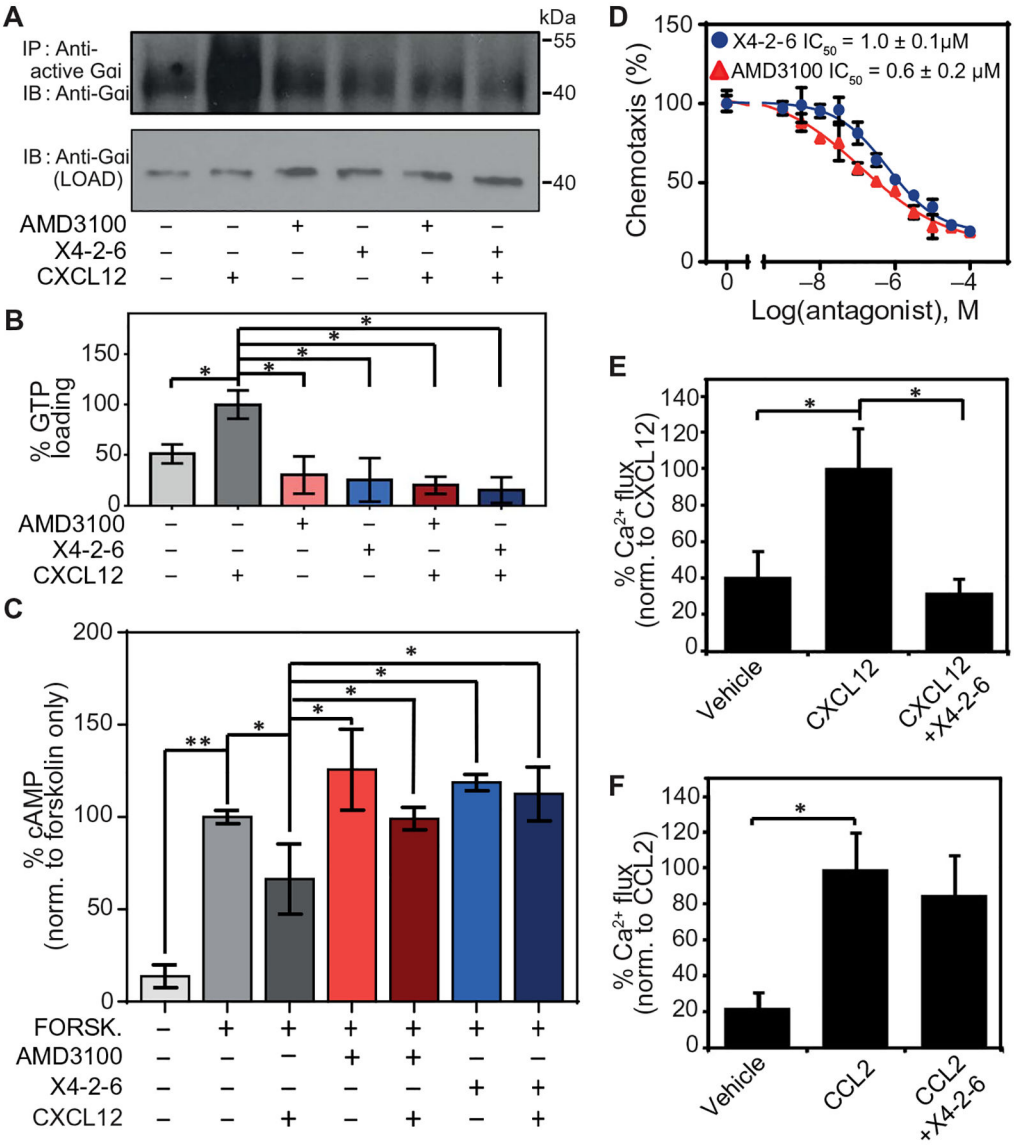


**Fig. 3. X4-2-6 specifically inhibits G protein activation downstream of CXCR4.**

(**A** and **B**) Western blotting analysis for the GTP loading of Gαi in Jurkat cells pretreated with vehicle, AMD3100, or X4-2-6 and stimulated with CXCL12. (A) Blots are representative of three independent experiments. IP, immuno-precipitation; IB, immunblotting. (B) Quantified data are means ± SD from all experiments. $*P < 0.01$ by ANOVA. (**C**) Enzyme-linked immunosorbent assay (ELISA)–based analysis of the intracellular concentrations of cAMP in Jurkat cells treated as indicated. Data are means ± SD of three independent experiments with six replicates per condition. $*P < 0.05$ and $**P < 0.005$ by Student's *t* test. (**D**) Transwell migration assay of Jurkat cell chemotaxis toward CXCL12 after treatment with AMD3100 or X4-2-6. Data are means ± SD of three independent experiments each performed in triplicate. (**E**) $Ca^{2+}$ flux analysis in THP-1 cells treated with vehicle or X4-2-6 and stimulated with CXCL12 as indicated. Data are means ± SD from 12 biological replicates. $*P \leq 5 \times 10^{-8}$ by Student's t test. (**F**) $Ca^{2+}$ flux analysis in

THP-1 cells treated with vehicle or X4-2-6 and stimulated with CCL2 as indicated. Data are means ± SD from 12 biological replicates. $*P \leq 5 \times 10^{-8}$ by Student's t test.

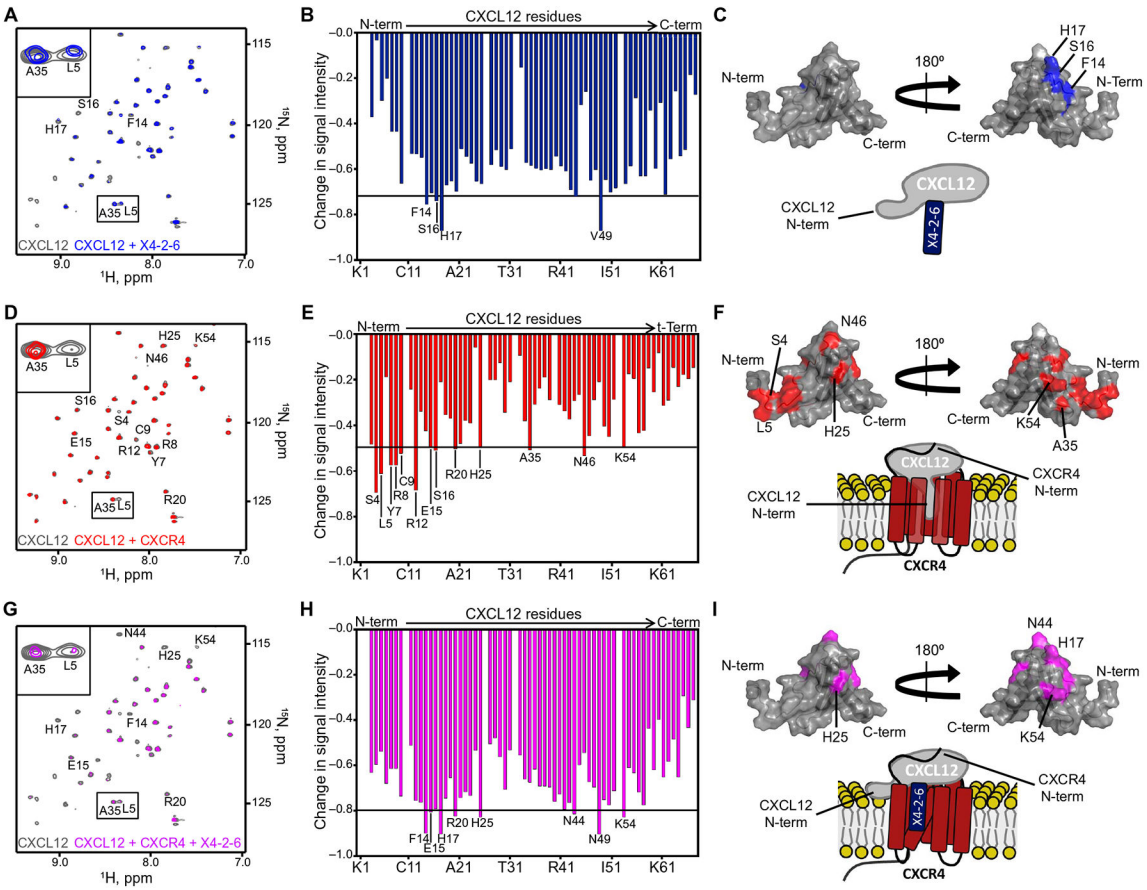


**Fig. 4. X4-2-6 forms a ternary complex with CXCL12 and CXCR4 to function as a biased antagonist.**

(**A** to **C**) NMR spectroscopy analysis of CXCL12 alone (gray) and in the presence of X4-2-6 (blue). Peak superimposition (A) and changes in CXCL12 HSQC signal intensity caused by the addition of X4-2-6 (B) are representative of two independent experiments. ppm, parts per million. (C) Substantially altered residues are mapped onto the NMR structure of CXCL12 (Protein Data Bank ID: 2KEE), and the cartoon models the interaction between the N-loop of CXCL12 and X4-2-6. (**D** to **F**) NMR spectroscopy analysis of CXCL12 alone (gray) and with membrane preparations containing CXCR4 (red). Peak superimposition (D) and changes in the signal intensity of CXCL12 residues caused by the addition of CXCR4 (E) are representative of two independent experiments. (F) Substantially altered residues are mapped onto the structure of CXCL12, and the cartoon models the interaction involving insertion of the N terminus of the chemokine into the receptor transmembrane helical bundle. (**G** to **I**) NMR spectroscopy analysis of CXCL12 alone (gray) and with CXCR4-containing membranes and X4-2-6 (magenta). Peak superimposition (G) and changes in CXCL12 signal intensity caused by the addition of CXCR4 and X4-2-6(H) are representative of two independent experiments. (I) The most substantial changes are mapped onto the NMR structure of CXCL12, and the cartoon models X4-2-6 binding to CXCR4 and CXCL12 to partially inhibit the binding of the extreme N terminus of the chemokine to the receptor.

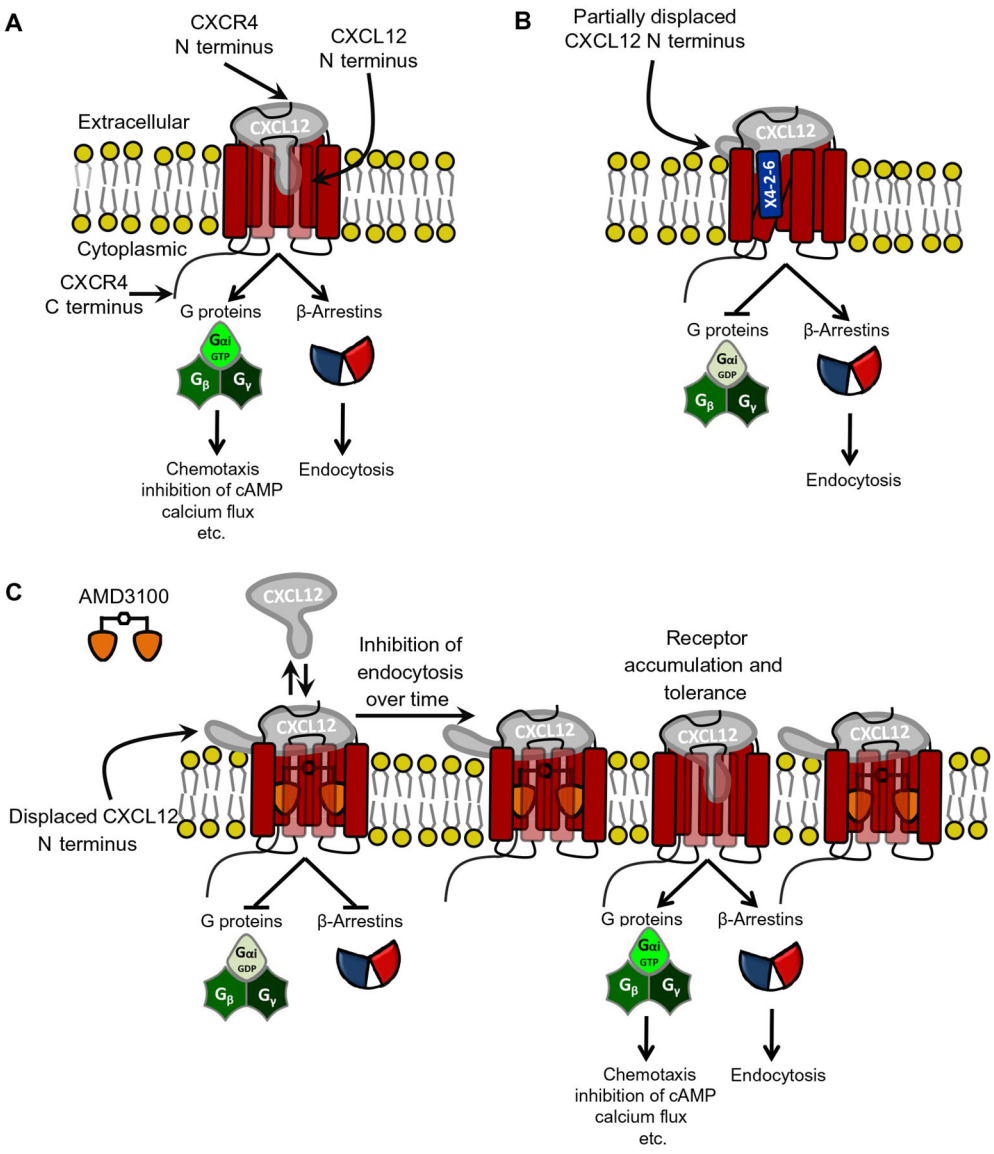


**Fig. 5. Proposed model for the mechanism of biased antagonism and development of tolerance to unbiased antagonists.**

**(A)** The current paradigm of CXCL12-mediated CXCR4 signaling suggests that the CXCL12 N terminus and N-loop insert into the CXCR4 transmembrane helical bundle, whereas the receptor N terminus binds to the globular domain of the chemokine. This leads to the activation of CXCR4 and subsequent G protein signaling, BA1/2 recruitment, and receptor endocytosis. (**B**) Our data suggest that X4-2-6 binds to CXCL12 and CXCR4 to form a ternary complex and displaces the extreme N-terminal portion of CXCL12 away from the transmembrane helical bundle of CXCR4. Thus, X4-2-6 functions as a biased antagonist by inhibiting G protein signaling but not BA1/2 recruitment to CXCR4. (**C**) In contrast, AMD3100 displaces the entire CXCL12 N terminus to inhibit all CXCR4 signaling. Over time, the inhibition of BA1/2 and the subsequent endocytosis result in the

accumulation of CXCR4 on the cell surface, CXCL12 binding to the receptor, and the development of tolerance to AMD3100. GDP, guanosine diphosphate.